

Knee Exoskeleton Assistive Torque Control Based on Real-Time Gait Event Detection

Dongfang Xu[✉], Xiuhua Liu, and Qining Wang[✉], *Senior Member, IEEE*

Abstract—In this paper, an assistive torque control strategy is proposed for the control of a bionic knee exoskeleton based on real-time gait event detection. Real-time gait event detection is executed with an inertial measurement unit based on an onboard trained model. Two models are trained based on the collected data from the knee exoskeleton at normal walking speed under zero torque and assistive torque control modes, respectively. We conduct two experiments: 1) real-time detection experiments under zero torque control at different speeds and 2) real-time detection and assistive torque control experiments based on real-time detection results at different speeds. Five able-bodied subjects participated in the experiments. The recognition accuracy and assistive torque performances based on real-time detection are evaluated. The experimental results show that all the critical gait events are detected rightly and the delay of gait event detection does not lead to damage to the overall system of knee exoskeleton. In addition, in real-time detection and assistive torque control experiments, parameters of the controller are refreshed for the current cycle based on the previous gait cycle, which is reasonable according to the detection result. The tracking performance of the torque could meet the requirement. This paper provides a feasible and applicable method for knee exoskeleton control based on real-time gait event detection.

Index Terms—Knee exoskeleton, assistive torque control, real-time gait event detection.

I. INTRODUCTION

PEOPLE with muscle weakness or impairments fail to fully accomplish daily activities. One way to solve the problem is to supply assistive torque with an external device. Recently, increasing attentions have been paid to lower-limb exoskeleton for its functions [1]–[3]. Knee exoskeleton plays an important role in assisting individual's daily activities, such as sit, stand and walking [4], [5], since it can provide supportive assistance/resistance.

Manuscript received April 30, 2019; accepted May 31, 2019. Date of publication July 23, 2019; date of current version August 21, 2019. This paper was recommended for publication by Associate Editor L. Zollo and Editor P. Dario upon evaluation of the reviewers' comments. This work was supported in part by the National Key Research and Development Program of China under Grant 2018YFB1307302 and Grant 2018YFF0300606, in part by the National Natural Science Foundation of China under Grant 91648207, in part by the Beijing Natural Science Foundation under Grant L182001, and in part by the Beijing Municipal Science and Technology Project under Grant Z181100009218007. (Dongfang Xu and Xiuhua Liu contributed equally to this work.) (Corresponding author: Qining Wang.)

The authors are with the Robotics Research Group, College of Engineering, Peking University, Beijing 100871, China, also with the Beijing Innovation Center for Engineering Science and Advanced Technology, Peking University, Beijing 100871, China, and also with the Beijing Engineering Research Center of Intelligent Rehabilitation Engineering, Beijing 100871, China (e-mail: qiningwang@pku.edu.cn).

Digital Object Identifier 10.1109/TMRB.2019.2930352

Various control methods for exoskeletons have been proposed [6]. These approaches can be divided roughly into three types according to control objectives: position control, impedance control and torque control. Position control [7]–[9] is to control the angle to a desired position and more likely to assist human's motion to apply a predefined joint angle trajectory, which is especially helpful when the wearer has limited residual motor functions [1]. Impedance control [3], [10]–[13] is an approach to control the relationship between the accepted angle/angular velocity and the yielded torque in the scope of mechanical rotation. It acts based on the wearer's performance and operates under the principle of assistance-as-needed, which is effective for assistance in gait rehabilitation. Torque control is widely used in exoskeletons [14]–[16]. There are two different torque control strategies commonly applied: open-loop torque control and closed-loop torque control. For open-loop torque control: a pre-specified torque curve is applied according to the assumed phase of the gait cycle (GC). For closed-loop torque control: the torque is proportionally applied based on a specific sensor such as a force sensor between the wearer and the exoskeleton. However, to assist walking safely and conveniently, the control strategy should be made according to human motion intents. Therefore, the detection of human's motion intent should be combined with control strategy.

Gait event detection has attracted intensive attentions for its importance in exoskeleton control [1], [6]. Foot pressure can be widely used in gait analysis to detect swing and stance efficiently [17], [18]. It is measured by pressure sensor (force sensitive resistors) which is susceptible to mechanical failure and has limited durability. Besides, pressure sensors are extra separated sensory apparatuses relative to knee exoskeleton, which will bring inconvenience in user wearing. Some other sensing methods are also used to detect gait event by attaching the electrodes of sensors on the limb, e.g., Electromyography (EMG) signals [19]–[21] and noncontact capacitive sensing [22]. In addition, mechanical sensors (e.g., accelerometer [23], gyroscope [24], inertial measurement unit (IMU) [25]) are also widely used in exoskeleton studies. These mechanical sensors which are easily integrated with exoskeletons, can provide acceleration information (e.g., accelerometer), angular velocity (e.g., gyroscope), or both acceleration and angular velocity information (e.g., IMU) during the whole gait cycle.

Several recent studies discussed the control of knee joint exoskeleton based on gait events [14], [26], [27]. Huo *et al.* [14] and Wehbi *et al.* [27] conducted exoskeleton

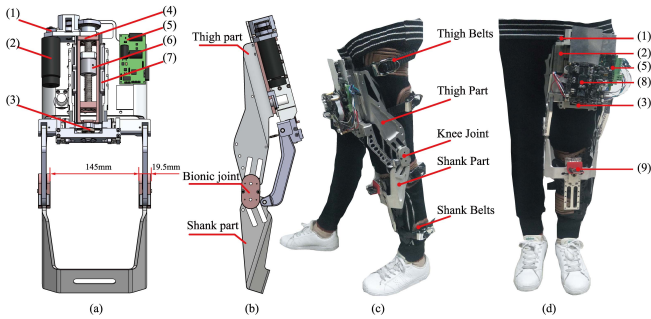


Fig. 1. The mechanical design schemes and wearing diagrams of knee exoskeleton. (a) and (b): the mechanical design schemes of the knee exoskeleton. (a)The transmission, sensory and control components are labeled: (1) Two-stage Belt drive, (2) High-power DC motor, (3) Force sensor, (4) Fixed frame, (5) Motor driver board, (6) Ball screw, (7) Rail & slider and (8) Control circuit board. (b) The actuator is fixed to the thigh, with the output extending down to the shank; (c) and (d): the wearing diagrams of knee exoskeleton. (9) IMU.

control based on gait events. The detection was based on the pressure insole. The subjects were asked to walk at quite low speeds (i.e., lower than their normal speeds) during experiments. Li *et al.* developed gait assistance control of a lower-extremity (hip-knee) assistive device for level-ground walking under slow speeds (1 km/h, 1.5 km/h and 2 km/h) based on gait event detection [26]. The detection was based on resistive force sensors which may bring the wearing inconveniences and integration difficulties. In addition, the detection existed errors and their off-line training process was tedious [26].

To solve the existed challenges (wearing, system integration and detection accuracy) of knee exoskeleton, we conduct the research on the control of a bionic knee exoskeleton based on real-time gait event detection at different speeds. In this study, a bionic knee exoskeleton is designed and a three-level assistive torque control method for the knee exoskeleton is proposed. A real-time detection method for gait event with one IMU is proposed in high-level controller based on the onboard training of model with Support Vector Machine (SVM) classifier. Adopted from the biomechanical analysis [28], the control strategies are designed based on three gait events in mid-level controller and assistive torque is exerted on the knee exoskeleton in low-level controller. Closed-loop torque control and open-loop torque control are applied to provide assistance and produce braking torque, respectively. To evaluate the performance of the overall system, online experiments with assistive torque control and zero torque control are conducted.

The rest of this paper is organized as follows. Section II introduces the bionic knee exoskeleton, the control method, experimental protocol and evaluation method. Experimental results are presented in Section III. Discussion and conclusion are demonstrated in Sections IV and V, respectively.

II. METHOD

A. Bionic Knee Exoskeleton

The bionic knee exoskeleton used in this study is shown in Fig. 1 and its detailed parameters are listed in Table I. The knee joint may be simply modeled as a pin-joint which

TABLE I
THE BIONIC KNEE EXOSKELETON PERFORMANCE

Item	Performance
Peak torque (cont.)	64 Nm
Peak torque(short time(~ 2 s))	96 Nm
Range of Motion	$-5^\circ \sim 135^\circ$
Back driving torque	$-15 \sim 17$ Nm
Backlash	$< 1^\circ$
Weight without Battery	2.1 kg

has only one DOF with a fixed rotation axis. However, knee joint has a nonuniform geometry with varying articulating surfaces and a nonconstant rotation axis. To design the joint of a lower-extremity knee exoskeleton, the natural knee kinematics should be considered. Then there is a tradeoff between natural joint and robotic joint. Here we adopt a pure rolling structure to reduce kinematic complexity to a tractable form. The rotation center of the proposed knee joint is the meshing point of the thigh gear and shank gear. It can move along the reference circle of thigh gear in pace with rotation of the shank. For the joint design, a rolling structure substitutes a simple hinge to approximately mimic the anatomic knee joint.

The knee exoskeleton is made of aluminum. Its whole weight is about 2.1 kg including the control board, sensors and motor, but without battery. A self-designed brushless motor driver is used and the motor has an inline rotation encoder for motion control. The peak torque of motor is 64 Nm for long time use and 96 Nm for short time use. The range of knee joint motion is $-5^\circ \sim 135^\circ$. The backdrivability of the system is $-15 \sim 17$ Nm. The backlash is less than 1° . The transmission process is realized as follows. First, the brushless DC motor with rated power 200 W, rated voltage 24 \sim 48 V, rated current 30 A and peak time 2 s (EC-4 polo 30, Maxon Motor, Switzerland) drives an initial double-stage timing belt transmission (each stage 40 : 14). Then the belt transmission drives a 12 \times 4 mm lead ball screw in which the screw nut completes linear motion under the rack-slider structure. Consequently, the push force is transferred to a linkage mechanism structure. Finally, the force is transmitted to make the knee joint accomplish flexion and extension.

To obtain more useful information about the interaction between the wearer and the exoskeleton, positions of sensors are selected carefully. A bilateral load cell (FUTEK Inc., USA) mounted on the push rod is used to measure the interaction force between the wearer and the exoskeleton, where the force is acquired through an ADC module. Only one IMU is placed on the shank part of exoskeleton. The IMU can output gait information including triaxial angles, accelerations and angular velocities. In addition, the performance of the control circuit (the sample frequency is 100 Hz) can affect the onboard training and real-time detection remarkably. Here the designed system consists of a Micro Controller Unit (MCU) and an Application Processor Unit (APU). The implementation of MCU is based on a 216 MHz Cortex-M7 processor. The APU is primarily constructed with an integrated programmable SoC chip, which consists of two parts: a 667 MHz Cortex-A9 MPCore-based processing system (PS) and an FPGA-based

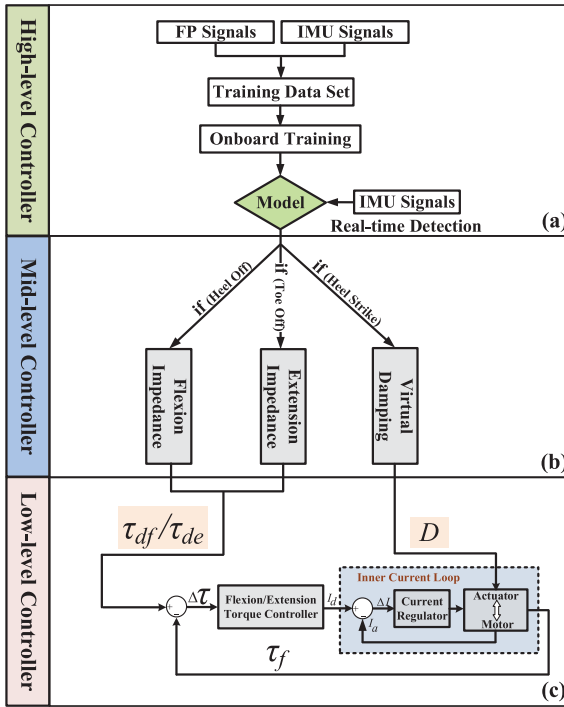


Fig. 2. A three-level control method of the knee exoskeleton. (a) High-level controller: used to train model on board and detect gait event in real time. (b) Mid-level controller: used to generate the control curve based on the gait event detection result. (c) Low-level controller: used to deliver the control curve to the actuator and next provide assistance to the exoskeleton.

programmable logic (PL) circuits. The MCU is used to collect and synchronize the sensors signals, and then packs them to APU. The APU is designed to execute onboard training and real-time gait event detection, and then outputs the detection result to MCU to execute control.

B. Control Method

A three-level controller is designed as shown in Fig. 2. The high-level controller is used to detect the gait event, then the corresponding control strategy is adopted based on the detection result in the mid-level controller, and finally the corresponding assistive torque is exerted on the knee exoskeleton in the low-level controller.

1) High-Level Controller: The high-level controller is used to train model and detect gait event, as shown in Fig. 2(a). In the study, IMU includes a tri-axis gyroscope and a tri-axis accelerometer. With embedded algorithm, it can provide the information of inclination angle (yaw, pitch and roll), a tri-axis acceleration and a tri-axis angular velocity. Excluding one channel (yaw) that is affected by the earth magnetic field, the signals of 8 channels (pitch, roll, tri-axis acceleration and tri-axis angular velocity) are used to train model and detect gait event. In this study, the pressure sensors in the shoe are used to record foot pressure (FP) signals just for the on board training. Notably, after the training has been finished and the trained model has generated, the subjects do not need to wear pressure sensors in the real-time gait event detection.

To acquire more effective information, some features of raw IMU signals are extracted by a continuous sliding window

(60 ms) with a 10 ms sliding increment. Five kinds of time-domain features are chosen according to the following expressions: $f_1 = \text{mean}(X)$, $f_2 = \text{std}(X)$, $f_3 = \max(X)$, $f_4 = \min(X)$ and $f_5 = \text{sum}(\text{abs}(\text{diff}(X)))$, where X is the raw data matrix of one sliding window, and it consists of six raw data vectors (since the size of sliding window is 60 ms in the study) and each raw data vector includes 8-channel signals. So the size of X is 6×8 . The $\text{mean}(X)$ and $\text{std}(X)$ are the mean value and standard deviation of all elements corresponding to each column in X , respectively. The $\max(X)$ and $\min(X)$ are the maximum and minimum of all elements corresponding to each column in X , respectively. The $\text{diff}(X)$ is the difference value of two adjacent elements of each column in X . The abs is the absolute value of each element and the sum is the summation of all elements corresponding to each column. All the feature values are concatenated to be a feature vector x , and the dimension of x is 40 (five features of each signal and there are 8-channels signals in total).

In onboard training, pressure sensor can record the pressure signals of the foot. When people wear foot pressure sensors, the foot pressure is close to 0 in swing phase and obviously higher than 0 in stance phase. By analyzing the toe pressure, heel pressure and the pressure summation of the whole foot, stance phase 1 (S1: from Heel Strike to Heel Off), stance phase 2 (S2: from Heel Off to Toe Off) and swing phase (SW: from Toe Off to Heel Strike) can be detected. Feature vectors with their specific labels (S1, S2 or SW) measured by the foot pressure signals form the training data set to train model. When the training is finished, the model will be output for the next real-time detection. The model describes the relations between the (sensor signal) feature vector and their labels (S1, S2 or SW). The training of model is the precondition for gait event detection, since the gait event detection is based on the model.

In real-time gait event detection, to get the detection result, the trained model need exist. The features of raw IMU signals are also extracted to form a feature vector in each sliding window. Each feature vector is fed to the trained model per sample interval in time series, and then the real-time detection result is output. The input of the model is the feature vector, and the output of model is S1, S2 or SW. The transition points from SW to S1, S1 to S2 and S2 to SW are corresponding to Heel strike, Heel Off and Toe Off.

Gait event detection can be viewed as data classification. Classification algorithm directly affects the detection accuracy. SVM is widely used in gait classification (detection) [29], [30]. The core of SVM is to construct an optimal hyperplane to separate the data belonging to different classes or labels. Its discriminant function can be seen as follows:

$$f(x) = \text{sgn} \left(\sum_{i=1}^N \alpha_i y_i K(x_i, x) + b \right) \quad (1)$$

where $K(x_i, x)$ is the kernel function of SVM, N is the number of support vectors, x_i is the i_{th} support vector, x is an input feature vector for real-time detection, α_i is the coefficient corresponding to support vector x_i , y_i is the label (corresponding

to S1, S2 or SW) of support vector of x_i , and b is a constant term. In the study, a radial basis function is chosen as the kernel function of SVM to execute onboard training and detection. It is shown as follows:

$$K(x_i, x) = \exp(-\gamma \|x_i - x\|^2) \quad (2)$$

where γ is a coefficient and $\gamma = 1/n$ (n is the dimension of the feature vector x and is 40 in this study).

The core of SVM is to construct an optimal hyperplane to separate the data belonging to different classes or labels. The hyperplane is built by simultaneously maximizing the boundary margin between two classes and minimizing the training classification errors. In the study, a multi-class SVM with “one-versus-one” structure is used. As the training data are labeled as S1, S2 or SW, the number of class is 3 in the study. For the three-class classification problem, three (C_3^2) binary classifiers are constructed based on “one-versus-one” structure. Three hyperplanes between any two classes are computed and built on board by iteration and optimizing with training data. For real-time detection, feature vector x is input to the individual binary classifiers. Therefore, there will be three detection decisions made based on the three binary classifiers. There is a vote rule to decide the final detection result: The class with the most occurrence number out of the three decisions is considered to be the final detection result, and if more than one class has the same number, the class with the smaller class index will be chosen as the detection results. The three binary classifiers and vote rule consist of the model, which is used in real-time detection.

The functions of high-level controller can be summarized as onboard training of model and gait event detection. Onboard training is building a model based on SVM for next detection. Real-time detection is that feature vector is fed to the trained model per sample interval in time series and detection result is output continuously.

2) Mid-Level Controller: Assistive control strategy is proposed based on gait event for providing assistance/resistance to the wearer while walking on the treadmill. The knee joint has two functions during walking: (1) Shock absorption as the limb is loaded and extensor stability for secure weight bearing in stance phase and (2) Rapid flexion in the initial swing phase for the limb advancement [31]. There are several critical moments in one GC: Heel Strike (the start of GC, i.e., 0%), Heel Off (40% of GC), Toe Off (64% of GC), the maximum flexion (70% of GC), the maximum extension (97% of GC) and the next Heel Strike (the end (100%) of GC and the start of next GC) [31]–[33]. Therefore, to supply appropriate assistance for the whole gait cycle, one gait cycle is divided into three gait phases: stance phase 1 (S1: from Heel Strike (0% of GC) to Heel Off (40% of GC)), stance phase 2 (S2: from Heel Off to Toe Off (64% of GC)) and swing phase (SW: from Toe Off (64% of GC) to Heel Strike (100% of GC)) as shown in Fig. 3.

In assistive control mode (AM), three assistive strategies are used to provide the necessary assistance/resistance for people wearing knee exoskeleton: virtual damping (VD), flexion impedance (FI) and extension impedance (EI) based on the detected gait phase as shown in Fig. 2(b). Stance phase

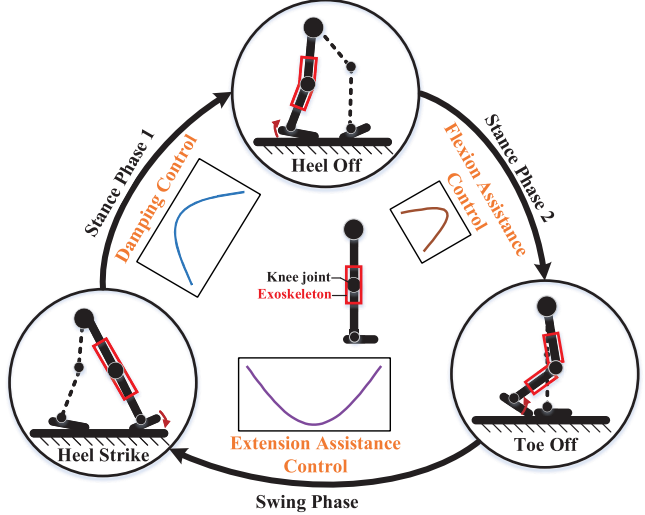


Fig. 3. Three critical gait events in one gait cycle: Heel Strike (the heel first contact the treadmill) at the start of the gait cycle, Heel Off (the heel first lift the treadmill), Toe Off (the toe first lift the treadmill) and the next Heel Strike at the end of the gait cycle. The S1 is from Heel Strike to Heel Off, the S2 is from Heel Off to Toe Off and the SW is from Toe Off to the next Heel Strike. The dashed line represents the sound leg (without the exoskeleton), the solid line represents the leg wearing the exoskeleton and the red box means the exoskeleton. The solid black circle means the joint. The division of gait events is based on the leg wearing the exoskeleton.

contains S1 and S2. To enhance the passivity of the knee joint [15], [34], a virtual damping control strategy is used in S1 [35], [36]. A flexion impedance control strategy is used to help the limb flex in S2.

Swing phase contains several subphases. The period from Toe Off (64% of GC) to the maximum flexion (70% of GC), and the period from the maximum extension (97% of GC) to Heel Strike (100% of GC) are relative small to the period from Toe Off (64% of GC) to Heel Strike (100% of GC) [31]–[33]. In swing phase, knee joint extends from the maximum flexion (70% of GC) to the maximum extension (97% of GC), which accounts for 75% (i.e., (97%-70%)/(100%-64%)) of the overall swing phase. Therefore, to simplify the control strategy in the preliminary research, the extension control is adopted during the whole period from Toe Off to Heel Strike to help the limb complete advancement and prepare for foot contact at the end of SW. In addition, the exoskeleton is in zero-torque mode (ZTM) (i.e., the desired torque (torque set-point) in the torque controller is zero) when the assistance/resistance is not necessary.

The assistance/resistance based on the real-time gait event detection related to the three control strategies are determined according to the following methods:

a) VD: To produce resistive torque of the knee without motor drive during the period from heel strike to heel off, an open-loop damping control strategy is adopted to adjust knee impedance, which has been achieved in the previous study on active transtibial prosthesis by our group [35]. If the motor-winding-short is switched on/off with a pulse width modulation (PWM) signal in an appropriate frequency, the braking torque will be positively correlated with the duty cycle (D) of the PWM signal and the resulting equivalent braking

torque τ_{eb} can be approximated as:

$$\tau_{eb} = k_d D n \quad (3)$$

where k_d is the proportionality coefficient in the unit of Nm/(r/min), D determines the relationship between the torque and the speed, it can be regarded as the damping coefficient and is in %, n is the rotate speed of the motor and is in r/min.

To generate appropriate braking torque, D is composed of a scaled sinusoid for S1 in this research. The D profile starts from the moment that the Heel Strike is detected and ends with the moment that the Heel Off is detected. The D based on VD is calculated as follows:

$$D = A_1 \sin(\pi P_{td}) \quad (4)$$

$$T_1 = \begin{cases} T_{1\min}, & T_1 < T_{1\min} \\ T_{1\max}, & T_1 > T_{1\max} \end{cases} \quad (5)$$

$$P_{td} = \frac{E_{td}}{T_1} \quad (6)$$

where A_1 represents the maximum value of the damping profile and T_1 measured by the controller represents the period of the previous S1. E_{td} represents elapsed time from the moment that Heel Strike is detected to the current moment. $T_{1\min}$ and $T_{1\max}$ are determined in the pre-experiments.

b) FI: The flexion torque consists of a scaled sinusoid for S2. The flexion torque profile starts from the moment that the Heel Off is detected and ends with the moment that the Toe Off is detected. The flexion torque τ_{df} based on FI is calculated by

$$\tau_{df} = A_2 \sin(\pi P_{tf}) \quad (7)$$

$$T_2 = \begin{cases} T_{2\min}, & T_2 < T_{2\min} \\ T_{2\max}, & T_2 > T_{2\max} \end{cases} \quad (8)$$

$$P_{tf} = \frac{E_{tf}}{T_2} \quad (9)$$

where A_2 represents the maximum value of the flexion torque profile and T_2 measured by the controller represents the period of the previous S2. E_{tf} represents elapsed time from the moment that Heel Off is detected to the current moment. $T_{2\min}$ and $T_{2\max}$ are determined in the pre-experiments.

c) EI: The extension torque consists of a scaled sinusoid for SW. The extension torque profile starts from the moment that the Toe Off is detected and ends with the moment that the next Heel Strike is detected. The extension torque τ_{de} based on EI is calculated by

$$\tau_{de} = A_3 \sin(\pi P_{te}) \quad (10)$$

$$T_3 = \begin{cases} T_{3\min}, & T_3 < T_{3\min} \\ T_{3\max}, & T_3 > T_{3\max} \end{cases} \quad (11)$$

$$P_{te} = \frac{E_{te}}{T_3} \quad (12)$$

where A_3 represents the maximum value of the flexion torque profile and T_3 measured by the controller represents the period of the previous SW. E_{te} represents elapsed time from the moment that Toe Off is detected to the current moment. $T_{3\min}$ and $T_{3\max}$ are determined in the pre-experiments.

Notably, T_1 , T_2 and T_3 are estimated from the previous cycle in real-time control in this study, which is only suitable for

TABLE II
THE VALUES OF THE PARAMETERS FOR THE FIVE SUBJECTS

Subject	D (%)	$T_{1\min}$ (s)	$T_{1\max}$ (s)	$T_{2\min}$ (s)	$T_{2\max}$ (s)	$T_{3\min}$ (s)	$T_{3\max}$ (s)
1	78	0.5	0.7	0.5	0.7	0.2	0.4
2	78	0.5	0.7	0.5	0.7	0.2	0.4
3	78	0.5	0.7	0.5	0.7	0.2	0.4
4	78	0.5	0.7	0.4	0.6	0.3	0.5
5	78	0.5	0.7	0.4	0.6	0.3	0.5

the motion on a treadmill, where the movement is periodic or quasiperiodic. The values of $T_{1\min}$, $T_{1\max}$, $T_{2\min}$, $T_{2\max}$, $T_{3\min}$ and $T_{3\max}$ are listed in Table II.

3) Low-Level Controller: The low-level controller shown in Fig. 2(c) consists of a current loop and a torque controller. For S1, the calculated D is directly delivered to the actuator and then the motor is driven to output assistance/resistance. The motor behaves as a generator when the motor rotates, and the rotation will generate an induced voltage. If the stator windings of the brushless motor are shorted, the induced voltage will generate a current, and then the current will produce a braking torque that prevents the motor from rotating. If the motor-winding-short is switched on/off with a pulse width modulation (PWM) signal in an appropriate frequency, the braking torque will be positively correlated with the duty cycle of the PWM signal.

For S2 and SW, the torque controller is to accurately track a desired torque signal. The inputs of the torque controller are the desired torque τ_{df}/τ_{de} generated in the mid-level controller and the assistive torque τ_f calculated from the load cell. The output of the torque controller is the desired current I_d for the motor which is also one of the input of the inner current loop. The other input of the current loop is the motor current I_a . The inner current loop utilizes the difference value between the motor's current I_a and the calculated value I_d from the torque controller to generate assistive torque.

C. Experimental Protocol

Five healthy subjects (1 female and 4 males) with an average age of 27.6 ± 5.1 years, an average weight of 61.5 ± 8.5 kg and an average height of 171.6 ± 6.8 cm participated in the study. The detailed information of subjects could be seen in Table III. All subjects provided informed written consents and the experiments have been approved by the Local Ethics Committee of Peking University.

1) Pre-Experiments for Parameter Setting: Before the Pre-experiment, each subject completes free walking task on the treadmill for some time with the knee exoskeleton under ZTM to acclimate the device and determine the slow, normal and fast walking speeds as shown in Table III. In pre-experiment, subjects start to walk on the treadmill with the knee exoskeleton under ZTM at slow, normal and fast speeds for 3 minutes, respectively. After the pre-experiments, the parameters mentioned above (i.e., $T_{1\min}$, $T_{1\max}$, $T_{2\min}$, $T_{2\max}$, $T_{3\min}$ and $T_{3\max}$) used in the next formal experiments are determined at the normal speed for each subject.

TABLE III
DETAILED INFORMATION OF THE FIVE HEALTHY SUBJECTS

Subject	Gender	Age (year)	Weight (kg)	Height (cm)	Walking Speed		
					Slow (m/s)	Normal (m/s)	Fast (m/s)
1	F ¹	24	46.5	163	0.6	0.8	1.0
2	M ¹	28	66.2	169	0.6	0.8	1.0
3	M	27	64.0	181	0.6	0.8	1.0
4	M	36	63.4	170	0.6	0.8	1.0
5	M	23	67.5	175	0.6	0.8	1.1 ²

¹ F means Female and M means Male.

² Subject 5 could walk at 1.1m/s for his fast speed.

2) *Knee Exoskeleton Control Experiments:* The control of knee exoskeleton is based on gait event detection. In this study, real-time experiments are designed, which could be divided into two sessions: Session 1 and Session 2. In Session 1, the gait data are collected to trained model on board under ZTM (i.e., training under ZTM). Based on the trained model, two real-time test experiments are conducted: 1) Zero torque control experiments: real-time gait event detection under ZTM at different speeds (slow, normal and fast); 2) Assistive torque control experiments: Assistive torque control based on real-time gait event detection at different speeds (slow, normal and fast). In Session 2, the gait data are collected to trained model on board under AM (i.e., training under AM). Based on the trained model, two real-time test experiments are also conducted: 1) Zero torque control experiments and 2) Assistive torque control experiments which are similar to Session 1.

For onboard training, subjects are asked to walk on the treadmill at their self-selected normal speeds for collecting data under ZTM and AM to train models, respectively. The real-time detection starts as soon as the onboard training is finished. During the real-time detection, subjects are asked to walk on the treadmill at three different speeds (slow, normal and fast) under ZTM and AM, respectively. Notably, in zero torque control experiments, the zero torque control is adopted and does not depend on the gait event detection result. In assistive torque control experiments, the assistive torque control is adopted based on the gait event detection result.

D. Performance Evaluation

1) *Onboard Training and Detection Time:* The control for exoskeleton depended on the real-time detection result while the real-time detection was based on the onboard trained model. Therefore, the onboard training time and detection decision time could reflect the time response performance. In onboard training, continuous 20 gait cycles' data were used as training data set for each subject under ZTM and AM, respectively. The training process started as training data set was fed to the classifier and ended as the model was saved. The elapsed time for the training process was training time. The detection decision time was the period from the moment one feature vector was fed into the trained model to the moment the detection result was output. The sliding window increment was one sample interval (i.e., 10 ms). Then the proportion of detection decision time in 10 ms was an critical metric.

2) *Detection Accuracy:* In this study, the exoskeleton control was based on critical gait events. Therefore it was essential to detect the critical gait events accurately and timely. In one gait cycle, the Heel Strike, Heel Off and Toe Off occurred just once. The right detection for critical gait event was defined as follows: every critical gait event was detected without no more or less than one time in each gait cycle.

3) *Detection Delay:* To evaluate the proposed method, we need to analyze the delay time between the detection moment and the truly occurred moment. The delay time T_d was calculated by the following equation:

$$T_d = t_d - t_l \quad (13)$$

where t_l was the truly occurred moment (labeled by the insole pressure) and t_d was the corresponding detection moment. As T_d varied from subject to subject, we calculated a normalized delay time (delay proportion) PT as follows:

$$PT = \frac{T_d}{T_c} \times 100\% \quad (14)$$

where T_c was time of averaged one gait cycle. PT reflected the delay time's proportion in one gait cycle. The positive PT represented that the moment of detected critical gait event was behind the true critical gait event moment and the negative PT denoted the critical gait was detected ahead of the true occurred gait event moment.

4) *Control Performance:* In Equation (4), (7) and (10), the time P_{set} (T_1 , T_2 or T_3) used to calculate the gait phase (P_{td} , P_{tf} or P_{te}) in the current gait cycle (GC) was the period of S1, S2 or SW in the previous GC rather than the time P_{real} of S1, S2 or SW in the current GC. Therefore, to evaluate the reasonability of the method, we defined incompleteness (ICP) computed by

$$ICP = \frac{P_{set} - P_{real}}{P_{set}} \times 100\% \quad (15)$$

where P_{set} (T_1 , T_2 or T_3) was the time measured in S1, S2 or SW of the former GC and P_{real} was the time to complete the phase (S1, S2 or SW) of the current GC. The negative value represented that the setting curve in S1, S2 or SW had been finished before the motion accomplished. The positive value represented that the motion in S1, S2 or SW had been accomplished before the set curve finished. After calculating the ICP , it was used to calculated the setting value SV (the setting torque in S2 and SW, or the setting damping in S1) at the end of the motion according to the corresponding Equation (4), (7) or (10).

III. EXPERIMENTAL RESULTS

A. Onboard Training and Detection Time

The onboard training time and detection decision time could reflect the time response performance. The mean onboard training time under ZTM was 5.59 ± 1.4 s. The detection time was 1.88 ± 0.26 ms for five subjects based on the model trained under ZTM, the corresponding proportion was 18.8% relative to the sliding window increment (10 ms). The mean training time for five subjects under AM was 5.06 ± 0.61 s and the mean detection time for five subjects was 1.72 ± 0.17 ms

TABLE IV

DELAY PROPORTION PT (MEAN \pm SEM) OF GAIT EVENT DETECTION FOR ZERO TORQUE CONTROL BASED ON ZTM TRAINING AND AM TRAINING FOR FIVE HEALTHY SUBJECTS(%)

		Detected Gait Event		
Training Mode	Speeds	Heel Strike	Heel Off	Toe Off
ZTM	Slow	-0.9 \pm 0.8	0.5 \pm 0.6	0.7 \pm 0.7
	Normal	1.2 \pm 0.6	0.4 \pm 0.3	0.6 \pm 0.2
	Fast	1.7 \pm 1.4	1.7 \pm 0.5	0.3 \pm 0.6
AM	Slow	-0.3 \pm 0.6	1.7 \pm 0.8	0.0 \pm 0.2
	Normal	-0.2 \pm 0.2	0.8 \pm 0.5	0.4 \pm 0.3
	Fast	-0.6 \pm 1.6	0.7 \pm 0.7	0.6 \pm 0.5

¹ The positive value represents that the detected critical gait moment comes behind the true critical gait event moment and the negative value represents the critical gait is detected ahead of the true occurred gait event moment.

based on the trained model (the proportion was 17.2% relative to the sliding window increment (10 ms)).

B. Real-Time Detection

1) *Accuracy of Detection:* In one gait cycle, the critical gait events (Heel Strike, Heel Off and Toe Off) just occurred once in time series. More than one detection or less than one detection for specific gait event meant false detection. In all real-time detection experiments, all the critical gait events were detected rightly (the detection accuracy was 100%), namely no false detection, which was beneficial to knee exoskeleton control.

2) *Delay of Detection:* Besides the detection accuracy, the detection delay is also an important criteria for knee exoskeleton control. The delay proportion PT was listed in Table IV and V. In Table IV, the maximum delay proportions were 1.7% (ZTM, fast speed) for Heel Strike and Heel Off detections and 1.7% (AM, slow speed) for Heel Off detection, which represented they were detected behind time (positive value). In Table V, the maximum delay proportion (no sign into consideration) was -2.1% (ZTM, slow speed) for Heel Strike detection, which represented it was detected in advance (negative value).

We also conducted a paired t-test on average detection delay to test the statistical significance. Based on the trained model under ZTM, we compared the detection delay in different speeds under zero and assistive torque control with the delay in normal speed under ZTM. The statistical significance was as follows: for slow speed under assistive torque control ($p < 0.05$) and for other situations ($p > 0.05$). Based on trained model under AM, compared with normal speed under assistive torque control, there was no statistical significance ($p > 0.05$). A paired t-test on average detection delay based on different training mode for specific speed was also conducted ($p > 0.05$ for all speeds under the two different trained models).

C. Torque Performance of Knee Exoskeleton

1) *Actuator Performance Under Zero Torque Control:* To evaluate the response performance for torque tracking of the

TABLE V

DELAY PROPORTION PT (MEAN \pm SEM) OF GAIT EVENT DETECTION FOR ASSISTIVE TORQUE CONTROL BASED ON ZTM TRAINING AND AM TRAINING FOR FIVE HEALTHY SUBJECTS(%)

		Detected Gait Event		
Training Mode	Speeds	Heel Strike	Heel Off	Toe Off
ZTM	Slow	-2.1 \pm 1.0	0.6 \pm 0.8	-0.4 \pm 1.4
	Normal	-1.1 \pm 1.6	0.8 \pm 0.7	0.5 \pm 0.3
	Fast	-0.7 \pm 0.7	-0.3 \pm 1.2	0.6 \pm 0.4
AM	Slow	0.5 \pm 0.7	0.8 \pm 0.6	-0.1 \pm 0.3
	Normal	0.7 \pm 0.6	0.5 \pm 0.4	0.0 \pm 0.4
	Fast	0.2 \pm 0.3	0.2 \pm 0.3	0.4 \pm 0.5

¹ The positive value represents that the detected critical gait moment comes behind the true critical gait event moment and the negative value represents the critical gait is detected ahead of the true occurred gait event moment.

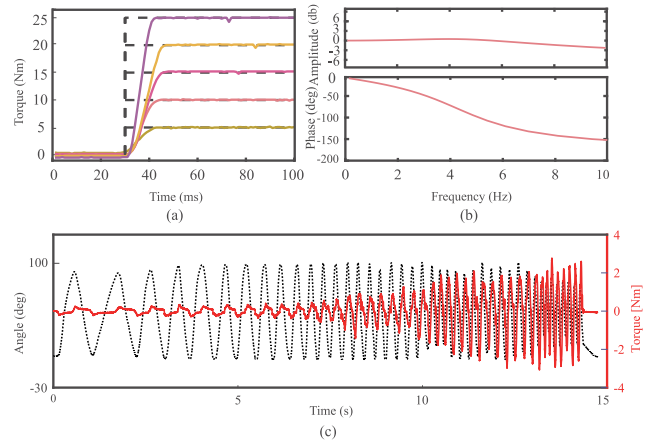


Fig. 4. (a) Step responses at 5, 10, 15, 20 and 25 Nm inputs. (b) The bandwidth of overall system between setting torque and output torque. (c) The transparency test of the knee exoskeleton: the dashed black line is the motion angle and the solid lines are the output torque.

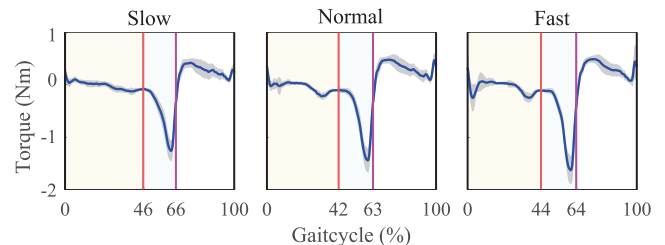


Fig. 5. The mean knee joint torque for one subject (subject 1) in a gait cycle in zero-torque mode at slow, normal and fast speeds, respectively. The solid black, red and purple lines represent Heel Strike, Heel Off and Toe Off, respectively. The solid blue line is the mean knee joint torque and the shade area is the standard deviation of knee joint torque.

exoskeleton, step response at 5, 10, 15, 20 and 25 Nm and torque bandwidth for 10 Nm were tested, which were shown in Fig. 4(a) and Fig. 4(b), respectively. It could be seen that the maximum torque response time was less than 20 ms for step response. The cutoff frequency was about 5 Hz.

The performance of transparency was important to the overall system and the experimental process of testing the

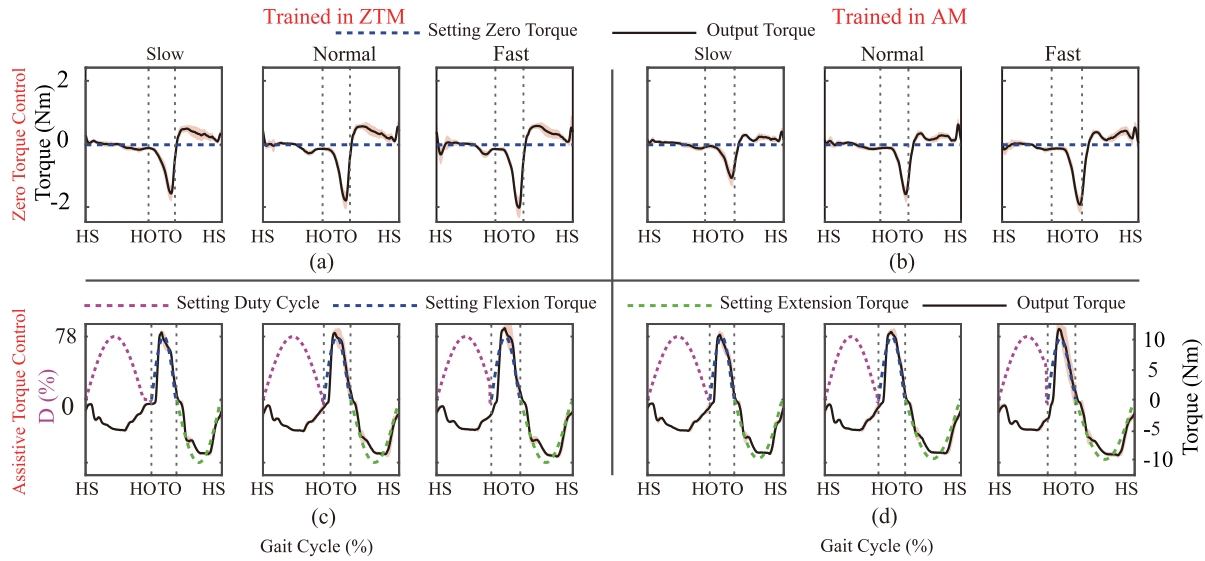


Fig. 6. The knee joint torque in one GC. (a) and (b) represent the performance of transparency of detection in ZTM in Session 1 and Session 2, respectively. The blue dashed line represents the setting torque and the black solid line represents the output torque measured by force sensor. (c) and (d) represent the assistive control performance of detection in AM in Session 1 and Session 2, respectively. The purple dashed line represents the duty cycle C . The blue dashed line represents the setting flexion torque and the green dashed line represents the setting extension torque. The black solid line represents the output torque measured by force sensor.

TABLE VI
THE MEAN $ICP(SV^1)$ (%) FOR FIVE SUBJECTS IN REAL-TIME DETECTION WITH ASSISTIVE CONTROL MODE UNDER ZTM AND AM

Control Mode	S1			S2			SW			
	Slow	Normal	Fast	Slow	Normal	Fast	Slow	Normal	Fast	
Trained in ZTM	Pressure ² IMU ³	-0.61(0) -0.44(0)	-0.47(0) -0.88(0)	-0.38(0) -1.67(0)	-0.24(0) -0.44(0)	-0.67(0) -0.43(0)	-0.75(0) -1.03(0)	-0.04(0) -0.38(0)	0.05(0.03) -0.14(0)	0.11(0.05) -0.44(0)
Trained in AM	Pressure IMU	0.04(0.22) -0.07(0)	-0.15(0) 0.04(0.22)	-0.22(0) -0.80(0)	-1.16(0) -0.78(0)	-0.49(0) -0.41(0)	-0.51(0) -0.31(0)	-0.05(0) -0.25(0)	-0.01(0) -0.04(0)	-0.15(0) -0.02(0)

The negative value represents that the setting curve in S1, S2 or SW has been finished before the motion accomplished. The positive value represents that the motion in S1, S2 or SW has been accomplished before the setting curve finished.

[1] SV is the setting value in the control curve when the motion is accomplished. The dimension of SV in S1 is (%); The dimension of SV in S2 and SW is (Nm);

[2] According to threshold value division method based on insole pressure;

[3] According to real-time detection results based on IMU.

transparency was as follows. Fix the thigh part of the knee exoskeleton so that the shank part of the knee exoskeleton was free to move. Under zero torque control, the shank part was manually controlled to complete the flexion and extension movement meanwhile the movement angle and torque information were collected. The torque and angle under ZTM were plotted in Fig. 4(c). The maximum error was less than 3 Nm at the fast frequency (about 5 Hz).

In addition, the movement characteristics under ZTM at three speeds were analyzed, which was shown in Fig. 5. Heel Strike was the start/end of one gait cycle. Heel Off was detected at 46%, 42% and 44% of one gait cycle corresponding to slow, normal and fast speeds. Toe Off was detected at 66%, 63% and 64% of one cycle corresponding to slow, normal and fast speeds. In addition, the maximum output torque was less than 2 Nm (no sign into consideration) at three speeds.

2) *Performance of Assistive Torque Control:* Fig. 6 depicted the knee joint torque in one GC in Session 1 and Session 2. Fig. 6(a) and Fig. 6(b) showed the performance of transparency under zero torque control in Session 1 and Session 2,

respectively. One could find that the torque tracking error increased as the walking speed increased. However, the maximum error was less than 2 Nm. The assistive control performance under assistive torque control in Session 1 and Session 2 was shown in Fig. 6(c) and Fig. 6(d), respectively. The resistant torque reached the maximum value (about -5 Nm) when the D in S1 reached the maximum at about half of S1. The output flexion torque reached the maximum value (about 10 Nm) at about half of S2 and the output extension torque reached the maximum value (about -10 Nm) at about half of SW. Fig. 6 demonstrated that the same gait events were detected at different percentages of gait cycle for different speeds.

The ICP in real-time detection with assistive control based on the trained model under ZTM and AM was shown in Table VI. As mentioned above, the ICP were calculated based on insole pressure and detection result, respectively. For calculation based on insole pressure: The ICP in S1 at slow speed, in which the model trained under AM, was a positive value 0.04%. The ICP in SW at normal speed and fast speed, in

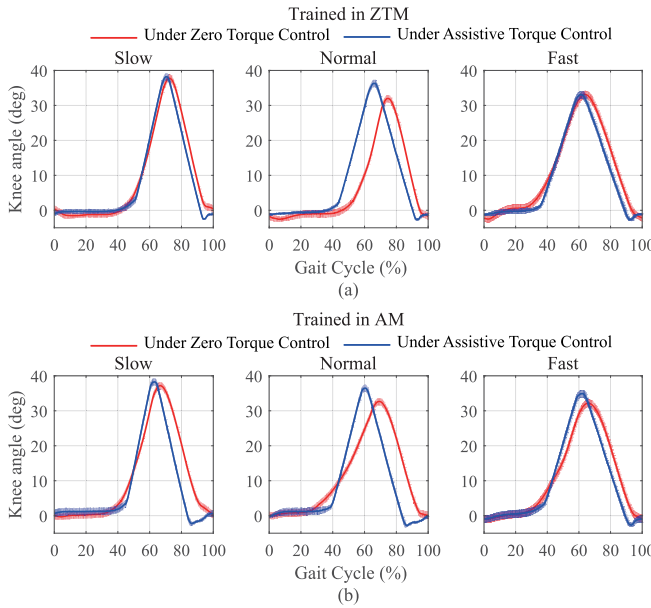


Fig. 7. Knee joint angle trajectories under zero torque control and assistive torque control. (a) The knee angle is tested under zero torque control and assistive torque control, in which the model is trained under ZTM at normal speed. (b) The knee angle is tested under zero torque control and assistive torque control, in which the model is trained under AM at normal speed.

which the models were trained under AM, were positive values 0.05% and 0.11%, respectively. For other situations, the *ICP* were all negative values and the minimum value occurred in S2 at slow speed, in which the model trained under AM was -1.16% .

For calculation based on detection result: The *ICP* in S1 at normal speed, in which the model was trained under AM, was a positive value 0.04% and the corresponding setting *D* was 0.22%. For other situations, the *ICP* were all negative values and the minimum value occurred in S1 at fast speed, in which the model was trained under ZTM, was -1.67% and the corresponding setting torque was 0 Nm.

3) Knee Joint Angle: The knee joint angles under zero torque control and assistive torque control were shown in Fig. 7. In real-time detection experiments based on the model that was trained under ZTM, the range of knee angle in assistive torque control was larger than the one in zero torque control at normal speed. And the range of knee angle tested in assistive torque control was similar to the one in zero torque control at slow or fast speeds. In real-time detection experiments based on the model that was trained under AM, the range of knee angle in assistive torque control was larger than it in zero torque control at slow, normal and fast speed respectively. Especially, the range of knee angle tested in assistive torque control was clearly larger than it in zero torque control at normal speed.

IV. DISCUSSION

In this paper, an assistive torque control method is proposed for a bionic knee exoskeleton based on real-time gait event detection. The control method consists of high-level controller, mid-level controller and low-level controller. A real-time detection method for gait event with one IMU is proposed in

high-level controller based on the onboard training of model with SVM. The control strategies are designed based on gait events in mid-level controller and assistive torque is exerted on the knee exoskeleton in low-level controller. To evaluate the performance of the overall system, five healthy subjects are recruited and online experiments with assistive torque control and zero torque control are conducted.

A. Onboard Training and Real-Time Detection

The onboard training time and real-time detection decision time reflect the time response performances of the system. In this study, the onboard training time are 5.59 s and 5.06 s corresponding to ZTM and AM, respectively. Onboard training under AM shows better time performance than it under ZTM. In addition, real-time detection is quite important. It should be shorter than the sliding window increment [37] (a sample interval in the study). The time for finishing per gait event detection are about 1.88 ms and 1.72 ms corresponding to different models (ZTM training and AM training), which is short enough compared with the sliding window increment 10ms. The proportions are about 18.8% and 17.2% corresponding to ZTM and AM. The detection time shows a fast response performance of the designed system.

In this study, three gait events (Heel Strike, Heel Off and Toe Off) are detected with 100% accuracy. Detection delay proportion *PT* could be seen in Tables IV and V. A paired t-test on average detection delay based on different training mode for specific speed is conducted ($p > 0.05$ for all speeds under the two different trained models). There is no statistical significance for the two trained models. In Table IV, the detection is conducted in zero torque control. Though there is some big delay proportion (*PT*) ($-0.9\% \pm 0.8\%$, $1.7\% \pm 1.4\%$, $1.7\% \pm 0.5\%$ and $-0.6\% \pm 1.6\%$), the existed delay occurs under zero torque control. The zero torque control is not based on critical gait event. Therefore, the delay in Table IV will not cause negative impact to zero torque control, which is acceptable.

In addition, what we care more about in real applications is the assistive torque control based on real-time gait event detection. The real-time detection can affect the assistive torque control performance. The study compares the delay proportion of real-time detection in assistive torque control under two training modes (ZTM and AM) as shown in Table V. Except for the situation (slow, Heel Off), the detection delay proportion (*PT*) based on model trained under ZTM is smaller than it trained under AM, for all other situations, the detection delay proportion based on model trained under AM is smaller than it trained under ZTM. For the proposed assistive control strategy, it is better if the delay proportion is closer to 0. The results prove that the detection performance based the model trained under AM is better than that based on the model trained under ZTM, which is beneficial to assistive torque control of the knee exoskeleton.

B. Performance of Torque Control

1) Zero Torque Control: As shown in Fig. 4(c), the transparency of the system is less than 3 Nm at the fast frequency,

which is comparable with [5]. In addition, as shown in Fig. 5, Fig. 6 (a) and Fig. 6 (b), when the subject was walking on the treadmill with wearing the exoskeleton in zero torque control, the maximum torque is nearly 2 Nm which is less than [38] (about 3.1 Nm).

2) *Assistive Torque Control*: As shown in Table VI, the *ICP* calculated based on detection result in S1 at normal speed is a positive value 0.04% (the model is trained under AM). Namely, in this situation, the motion is fully accomplished (100%) when the setting curve is finished 99.96%. The corresponding D is 0.22% which is very close to 0% that it should be. Therefore, the remained control curve may not lead to damage to the motion. For other situations, the *ICP* calculated based on detection result are all negative values and the minimum value occurring in S1 at fast speed is -1.67% (the model is trained under ZTM). Namely the setting curve has been fully finished (100%) when the motion is accomplished 98.33% and the corresponding setting value is 0. That's to say all motions could be accomplished over 98% when the setting curve has been fully finished (100%). In addition, the remained less than 2% motion is achieved under ZTM. Therefore, there won't be harm to the motion, that is to say, parameters refreshing (T_1 , T_2 and T_3) for control curve of the current cycle based on the previous gait cycle is reasonable.

C. Wearable Sensors for Gait Event Detection

For comparison, the *ICP* based on insole pressure is also calculated and shown in Table VI. There are two situations based on insole pressure or detection result: 1) P_{set} is larger than P_{real} ; 2) P_{set} is smaller than P_{real} .

For the situation where P_{set} is larger than P_{real} : For calculation based on detection results, it occurs only in S1 at normal speed, in which the model is trained under AM. *ICP* is 0.04% and the corresponding D is 0.22% which is very close to 0 that it should be. For calculation based on insole pressure, it occurs in three situations: (1) In S1 at slow speed, where the model is trained under AM, *ICP* is 0.04% and the corresponding setting D is 0.22% which is very close to 0 that it should be. (2) In SW at normal speed, where the model is trained under ZTM, *ICP* is 0.05% and the corresponding setting torque is 0.03 Nm which is very close to 0 Nm that it should be. (3) In SW at fast speed, where the model is trained under ZTM, *ICP* is 0.11% and the corresponding setting torque is 0.05 Nm which is very close to 0 Nm that it should be. Therefore, the effect is similar when P_{set} is larger than P_{real} whether they are calculated based on insole pressure or detection result.

For situation that P_{set} is smaller than P_{real} : For calculation based on insole pressure, the minimum *ICP* value occurring in S2 at slow speed is -1.16% (the model is trained under AM). For calculation based on detection result, the minimum value occurring in S1 at fast speed, in which the model is trained under ZTM is -1.67% . Therefore, the motions have been accomplished over 98% of them when the setting curve has been finished whether they are calculated based on insole pressure or detection result. Therefore, for gait event detection, IMU sensor could achieve comparable results with pressure

sensor for control, but with less challenges in mechanical failure and durability.

D. Detection Delay in Control

Since the exoskeleton control is based on accurate gait events, the delay of detection may affect the knee control. The delay of detection is the difference value between the truly occurred moment (labeled by the insole pressure) and the corresponding detection moment when the gait event is detected by IMU sensor, as shown in Table IV and Table V. Therefore, influence of detection delay on control could be attributed to the influence of wearing sensors (IMU sensor and pressure sensor) on control. As mentioned in Section IV-C, IMU sensor could achieve comparable results with pressure sensor for control. As a result, the delay of detection would not cause any bad impact to the overall system in this study.

E. Limitations

Though current results show the feasibility of the proposed method, there are still limitations in this study. First, current control parameters are derived from the previous gait cycle. To make the system more improved, they should be linked with the current gait cycle in the future. Second, one gait cycle is divided into three gait phases (Stance1, Stance2 and Swing) according to three gait events, i.e., Heel Strike, Heel Off and Toe Off in this study. Actually, to better control the device, more refined division may be adopted, for example the swing phase may be divided into more subphases (Toe Off to maximum flexion, the maximum flexion to the maximum extension and the maximum extension to Heel Strike). It may be useful for future applications on different terrains. Third, the obtained results are based on healthy subjects. For clinical validation and application, experiments will be further conducted on patients with knee joint weakness and specific control strategy should be designed according to the patient's body conditions.

V. CONCLUSION

In this paper, an assistive torque control method for knee exoskeleton is proposed based on real-time gait event detection. To evaluate the feasibility of the overall system, five healthy subjects participated in the experiments and walked on the treadmill at different speeds. The experimental results show that the real-time detection with IMU has no errors with low time delay, and the assistive torque control based on the detection result is effective and feasible which can meet the requirements. The main contributions are as follows: First, only one IMU is adopted to detect gait event, which improves the knee exoskeleton durability and decreases the wearing inconvenience. Second, the result of real-time detection is capable of providing functional gait assistance at knee joint of the subject with low delay and high accuracy under different speeds during level-ground walking.

ACKNOWLEDGMENT

The authors would like to thank the anonymous reviewers for their valuable suggestions. They would also like to thank

S. Zhang, Y. Zhou and J. Mai for their contributions in the experiments.

REFERENCES

- [1] A. J. Young and D. P. Ferris, "State of the art and future directions for lower limb robotic exoskeletons," *IEEE Trans. Neural Syst. Rehabil. Eng.*, vol. 25, no. 2, pp. 171–182, Feb. 2017.
- [2] S. Maggioni *et al.*, "Robot-aided assessment of lower extremity functions: A review," *J. Neuroeng. Rehabil.*, vol. 13, no. 1, p. 72, 2016.
- [3] S. Wang *et al.*, "Design and control of the MINDWALKER exoskeleton," *IEEE Trans. Neural Syst. Rehabil. Eng.*, vol. 23, no. 2, pp. 277–286, Mar. 2015.
- [4] K. Kamali, A. A. Akbari, and A. Akbarzadeh, "Trajectory generation and control of a knee exoskeleton based on dynamic movement primitives for sit-to-stand assistance," *Adv. Robot.*, vol. 30, no. 13, pp. 846–860, 2016.
- [5] M. K. Shepherd and E. J. Rouse, "Design and validation of a torque-controllable knee exoskeleton for sit-to-stand assistance," *IEEE/ASME Trans. Mechatronics*, vol. 22, no. 4, pp. 1695–1704, Aug. 2017.
- [6] T. Yan, M. Cempini, C. M. Oddo, and N. Vitiello, "Review of assistive strategies in powered lower-limb orthoses and exoskeletons," *Robot. Auton. Syst.*, vol. 64, pp. 120–136, Feb. 2015.
- [7] H. Vallery, E. H. F. van Asseldonk, M. Buss, and H. van der Kooij, "Reference trajectory generation for rehabilitation robots: Complementary limb motion estimation," *IEEE Trans. Neural Syst. Rehabil. Eng.*, vol. 17, no. 1, pp. 23–30, Feb. 2009.
- [8] O. Mazumder, A. S. Kundu, P. K. Lenka, and S. Bhaumik, "Multi-channel fusion based adaptive gait trajectory generation using wearable sensors," *J. Intell. Robot. Syst.*, vol. 86, nos. 3–4, pp. 335–351, 2017.
- [9] G. Colombo, M. Joerg, R. Schreier, and V. Dietz, "Treadmill training of paraplegic patients using a robotic orthosis," *J. Rehabil. Res. Develop.*, vol. 37, no. 6, pp. 693–700, 2000.
- [10] A. Duschau-Wicke, J. von Zitzewitz, A. Caprez, L. Luenenburger, and R. Riener, "Path control: A method for patient-cooperative robot-aided gait rehabilitation," *IEEE Trans. Neural Syst. Rehabil. Eng.*, vol. 18, no. 1, pp. 38–48, Feb. 2010.
- [11] H. Ma, C. Zhong, B. Chen, K. M. Chan, and W.-H. Liao, "User-adaptive assistance of assistive knee braces for gait rehabilitation," *IEEE Trans. Neural Syst. Rehabil. Eng.*, vol. 26, no. 10, pp. 1994–2005, Oct. 2018.
- [12] B. Koopman, E. H. F. van Asseldonk, and H. van der Kooij, "Estimation of human hip and knee multi-joint dynamics using the LOPES gait trainer," *IEEE Trans. Robot.*, vol. 32, no. 4, pp. 920–932, Aug. 2016.
- [13] V. Rajasekaran *et al.*, "Volition-adaptive control for gait training using wearable exoskeleton: Preliminary tests with incomplete spinal cord injury individuals," *J. Neuroeng. Rehabil.*, vol. 15, no. 1, p. 4, 2018.
- [14] W. Huo, S. Mohammed, Y. Amirat, and K. Kong, "Fast gait mode detection and assistive torque control of an exoskeletal robotic orthosis for walking assistance," *IEEE Trans. Robot.*, vol. 34, no. 4, pp. 1035–1052, Aug. 2018.
- [15] S. A. Murray, K. H. Ha, C. Hartigan, and M. Goldfarb, "An assistive control approach for a lower-limb exoskeleton to facilitate recovery of walking following stroke," *IEEE Trans. Neural Syst. Rehabil. Eng.*, vol. 23, no. 3, pp. 441–499, May 2015.
- [16] P. Beyl, M. V. Damme, R. V. Ham, B. Vanderborght, and D. Lefever, "Pleated pneumatic artificial muscle-based actuator system as a torque source for compliant lower limb exoskeletons," *IEEE/ASME Trans. Mechatronics*, vol. 19, no. 3, pp. 1046–1056, Jun. 2014.
- [17] A. Parri *et al.*, "Real-time hybrid locomotion mode detection for lower-limb wearable robots," *IEEE/ASME Trans. Mechatronics*, vol. 22, no. 6, pp. 2480–2491, Dec. 2017.
- [18] L. Yu, J. Zheng, Y. Wang, Z. Song, and E. Zhan, "Adaptive method for real-time gait phase detection based on ground contact forces," *Gait Posture*, vol. 41, no. 1, pp. 269–275, 2015.
- [19] N. Nazmi, M. A. A. Rahman, S. I. Yamamoto, and S. A. Ahmad, "Walking gait event detection based on electromyography signals using artificial neural network," *Biomed. Signal Process. Control*, vol. 47, pp. 334–343, Jan. 2019.
- [20] J. Rafiee, M. A. Rafiee, F. Yavari, and M. P. Schoen, "Feature extraction of forearm EMG signals for prosthetics," *Expert Syst. Appl.*, vol. 38, no. 4, pp. 4058–4067, 2011.
- [21] A. Phinyomark, F. Quaine, S. Charbonnier, C. Serviere, F. Tarpin-Bernard, and Y. Laurillau, "EMG feature evaluation for improving myoelectric pattern recognition robustness," *Expert Syst. Appl.*, vol. 40, no. 12, pp. 4832–4840, 2013.
- [22] E. Zheng, S. Manca, T. Yan, A. Parri, N. Vitiello, and Q. Wang, "Gait phase estimation based on noncontact capacitive sensing and adaptive oscillators," *IEEE Trans. Biomed. Eng.*, vol. 64, no. 10, pp. 2419–2430, Oct. 2017.
- [23] S. Khandelwal and N. Wickstrom, "Evaluation of the performance of accelerometer-based gait event detection algorithms in different real-world scenarios using the MAREA gait database," *Gait Posture*, vol. 51, pp. 84–90, Jan. 2017.
- [24] D. Gouwanda and A. A. Gopalai, "A robust real-time gait event detection using wireless gyroscope and its application on normal and altered gaits," *Med. Eng. Phys.*, vol. 37, no. 2, pp. 219–225, 2015.
- [25] E. D. Ledoux, "Inertial sensing for gait event detection and transfemoral prosthesis control strategy," *IEEE Trans. Biomed. Eng.*, vol. 65, no. 12, pp. 2704–2712, Dec. 2018.
- [26] J. Li, B. Shen, C.-M. Chew, C. L. Teo, and A. N. Poo, "Novel functional task-based gait assistance control of lower extremity assistive device for level walking," *IEEE Trans. Ind. Electron.*, vol. 63, no. 2, pp. 1096–1106, Feb. 2016.
- [27] F. E. Z. Wehbi, W. Huo, Y. Amirat, M. E. Rafei, M. Khalil, and S. Mohammed, "Active impedance control of a knee-joint orthosis during swing phase," in *Proc. IEEE ICORR*, Jul. 2017, pp. 435–440.
- [28] R. Riener, M. Rabuffetti, and C. Frigo, "Stair ascent and descent at different inclinations," *Gait Posture*, vol. 15, no. 1, pp. 32–44, 2002.
- [29] H. Huang, F. Zhang, L. J. Hargrove, Z. Dou, D. R. Rogers, and K. B. Englehart, "Continuous locomotion-mode identification for prosthetic legs based on neuromuscular-mechanical fusion," *IEEE Trans. Biomed. Eng.*, vol. 58, no. 10, pp. 2867–2875, Oct. 2011.
- [30] E. Zheng and Q. Wang, "Noncontact capacitive sensing-based locomotion transition recognition for amputees with robotic transtibial prostheses," *IEEE Trans. Neural. Syst. Rehabil. Eng.*, vol. 25, no. 2, pp. 161–170, Feb. 2017.
- [31] J. Perry, *Gait Analysis: Normal and Pathological Function*. Thorofare, NJ, USA: SLACK, 1992.
- [32] J. R. Brinkmann and J. Perry, "Rate and range of knee motion during ambulation in healthy and arthritic subjects," *Phys. Therapy*, vol. 65, no. 7, pp. 1055–1060, 1985.
- [33] E. Y. Chao, R. K. Laughman, E. Schneider, and R. N. Stauffer, "Normative data of knee joint motion and ground reaction forces in adult level walking," *J. Biomech.*, vol. 16, no. 3, pp. 219–233, 1983.
- [34] O. Unluhisarcikli, M. Pietrusinski, B. Weinberg, P. Bonato, and C. Mavroidis, "Design and control of a robotic lower extremity exoskeleton for gait rehabilitation," in *Proc. IEEE RSJ Int. Conf. Intell. Robot. Syst.*, 2011, pp. 4893–4898.
- [35] Q. Wang, K. Yuan, J. Zhu, and L. Wang, "Walk the walk: A lightweight active transtibial prosthesis," *IEEE Robot. Autom. Mag.*, vol. 22, no. 4, pp. 80–89, Dec. 2015.
- [36] Y. Feng and Q. Wang, "Combining push-off power and nonlinear damping behaviors for a lightweight motor-driven transtibial prosthesis," *IEEE/ASME Trans. Mechatronics*, vol. 22, no. 6, pp. 2512–2523, Dec. 2017.
- [37] K. Englehart and B. Hudgins, "A robust, real-time control scheme for multifunction myoelectric control," *IEEE Trans. Biomed. Eng.*, vol. 50, no. 7, pp. 848–854, Jul. 2003.
- [38] D. Zanotto, Y. Akiyama, P. Stegall, and S. K. Agrawal, "Knee joint misalignment in exoskeletons for the lower extremities: Effects on user's gait," *IEEE Trans. Robot.*, vol. 31, no. 4, pp. 978–987, Aug. 2015.